Eur Biophys J (1986) 13:139–155

European Biophysics Journal

Curvature-electric effect in black lipid membranes

Dynamic characteristics*

A. G. Petrov[1] and V. S. Sokolov[2]

[1] Liquid Crystal Group, Institute of Solid State Physics, Bulgarian Academy of Sciences, 72 Lenin Blvd, BG-1184 Sofia, Bulgaria
[2] Institute of Electrochemistry, Academy of Sciences of the USSR, 31 Leninski prospect, SU-117071 Moscow, USSR

Received May 21, 1985/Accepted August 5, 1985

Abstract. Upon periodical bending of a BLM, by means of oscillating hydrostatic pressure with sound frequency, the generation of an a.c. electric current with the same frequency can be observed under short circuit conditions. Previously, this phenomenon was attributed by us to a displacement current due to the oscillating flexoelectric polarization. The latter is proportional to the membrane curvature and depends on the lipid dipole moment and surface charge.

The theory of this effect is outlined here. Earlier results concerning dipolar and quadrupolar contributions to the total current are presented and new expressions about charge contributions are derived for the two basic regimes of free and blocked lateral lipid exchange.

Further, a systematic study of the frequency dependence of the amplitude and phase of the curvature-electric signal from a bacterial phosphatidylethanolamine/n-decane BLM is reported. Constant membrane curvature at each vibration frequency was assured by a calibration of the capacitance current observed with a small transmembrane voltage.

The frequency dependence of the curvature-electric current amplitude was characterized by two regions: low frequency plateau and high frequency slope, the boundary between them being about 160 Hz. Such behaviour suggested a switching of the mechanism of membrane polarization from free to blocked lateral lipid exchange. Frequency dependence of the phase shift was characterized by low frequency and high frequency plateaus and a gradual transition between them. From phase measurements on initially curved membranes the sign of the membrane flexo-coefficient was found to be negative.

The influence of some modifiers of the surface charge and surface dipole, as well as of the membrane conductivity, upon the value of the effect was studied. Surface charge was separately measured by the internal field compensation method under an ionic strength gradient. The membrane flexoelectric coefficient was evaluated and compared to the theoretical predictions. A conclusion was drawn that under the present experimental conditions the main contribution to the effect comes from the curvature-induced shift of the surface charge equilibrium.

Key words: Membrane curvature, flexoelectricity, lateral lipid exchange, displacement current generation, phosphatidylethanolamine/n-decane BLM

1. Introduction

The first experimental evidence that a black lipid membrane (BLM) could generate a.c. electric current under the action of an oscillating hydrostatic pressure difference was obtained some 10 years ago. In the paper of Passechnik and Sokolov (1973) this effect was called "a peculiar kind of piezoeffect" and in a subsequent paper (Ochs and Burton 1974) the term "subharmonic noise" was used. Later on (Petrov 1975; Petrov and Derzhanski 1976; Derzhanski et al. 1981) emphasis was made on the membrane *curvature* variations in such experiments and the effect was related to the flexoelectric polarization of the bent liquid crystalline structure of the membrane. Flexoelectricity, or curvature electricity is a fundamental mechanoelectric property of liquid crystals (Meyer 1969; de Gennes 1974). Flexoelectricity of membranes in the liquid crystal state was recently reviewed (Petrov 1984).

The phenomenological description of the curvature-electric effect is simple. One should use the

* Presented at the Tenth International Liquid Crystal Conference, 15–21 July 1984, York, UK

basic constitutive equation for the flexoelectric polarization per unit membrane area, P_s, as proportional to the sum of two principal membrane curvatures, $c_1 + c_2$,

$$P_s = f(c_1 + c_2), \tag{1.1}$$

where f is the flexoelectric coefficient measured in coulombs [C]. For spherical curvature, $c_1 + c_2 = 2/R$, where R is the radius of curvature of the membrane. In the case of time-dependent, oscillating curvature with angular frequency, ω

$$c_1 + c_2 = 2 c_m \sin \omega t, \quad c_m = 1/R_m. \tag{1.2}$$

The surface polarization, P_s, will also be time-dependent. Here we will assume that the polarization instantaneously follows the change in curvature, i.e.

$$P_s(t) = f \cdot 2c(t). \tag{1.3}$$

The general case will be considered below. The time-dependent polarization will result in a displacement current which can be measured under short circuit conditions in the external circuit by means of two electrodes immersed in the bathing electrolyte solutions. This current could be expressed in two different ways, yielding equivalent results. The first way is to calculate the current density as a time derivative of the mean *volume* polarization

$$P_v = P_s/d, \tag{1.4}$$

where d is the membrane thickness, and then to multiply it by the membrane area in order to get the total current:

$$I(t) = S \cdot i(t) = S \dot{P}_v(t) = 2f \frac{S}{d} \omega c_m \cos \omega t. \tag{1.5}$$

Because of the change in curvature the membrane area will also oscillate, but this effect will contribute to the higher harmonics of the current. From (1.5) the amplitude of the first harmonic is

$$I_\omega = 2f \frac{S_0}{d} c_m \omega, \tag{1.6}$$

where S_0 is the area of the planar membrane.

The second way is to use the expression for the potential jump across a polarized membrane

$$\Delta U = P_s/\varepsilon \varepsilon_0, \tag{1.7}$$

where ε is the mean dielectric constant of the membrane and ε_0 is the absolute dielectric constant, and to express the charge of the membrane capacitor as $Q = C \Delta U$. Then the current is

$$I(t) = \dot{Q} = \dot{C} \Delta U + C \Delta \dot{U}. \tag{1.8}$$

The membrane capacitance oscillates like the membrane area but this again makes no contribution to the first harmonic of the current, which is

$$I_\omega = 2f \frac{C_0}{\varepsilon \varepsilon_0} c_m \omega. \tag{1.9}$$

Equation (1.6) is identical to (1.4) in view of the planar capacitor expression

$$C_0 = \varepsilon \varepsilon_0 S_0/d. \tag{1.10}$$

Thus, measuring I_ω and separately determining C_0 and c_m, one can obtain experimentally the value of the phenomenologically introduced flexo-coefficient. The molecular theory of the membrane flexoelectricity was derived by Petrov and Derzhanski (1976), Petrov and Pavloff (1979) and summarized by Petrov (1984). In general, important contributions to the flexoelectric coefficient come from the first three electrical multipole moments of the lipid molecules: charge, dipole and quadrupole. Some aspects of the role of charges were discussed by Derzhanski et al. (1981). The experimental elucidation of the importance of the different contributions by means of variation of the electrical multipoles is of a great interest. This is one of the aims of the present study. A second important question is the dynamics of the establishment of the curvature-induced polarization with respect to the rates of transbilayer and lateral lipid exchange (Petrov 1984). Information about the dynamics is obtained here by studying the frequency dependence of the flexoelectric signal.

2. Materials and methods

Bacterial phosphatidylethanolamine *ex E. coli* (Koch Light) dissolved in n-decane at a concentration of 20 mg/ml was used as a membrane-forming solution. Black lipid membranes were formed on a 1 mm hole in a Teflon cup, immersed in a spectrophotometric glass cuvette, at room temperature. As a bathing electrolyte either unbuffered KCl, $10^{-2} - 1\,M$ (pH 6.2) or buffered KCl with higher or lower pH values was used (KH_2PO_4 pH 3.0; MES pH 6.0; *TRIS* pH 8.5; CHES pH 9.3; KH_2PO_4 pH 10.4). Surface charge of the BLM was also varied by adsorption of the ionic detergent cetyltrimethylammonium bromide (CTAB, Chemapol), added to the electrolyte as a $10^{-3}M$ water solution. Surface dipole moment was varied by adsorption of the dipole modifier phloretin (Serva), added as a $10^{-2}M$ solution in ethyl alcohol. In some experiments the membrane conductivity was also modified by addition of the ionic carrier nonactin ($10^{-3}M$ solution in ethyl alcohol).

Membrane curvature oscillations were excited by the method first employed by Passechnik and Soko-

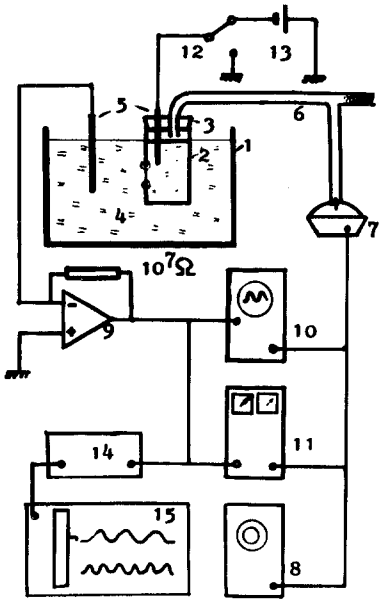

Fig. 1. Scheme of the experimental set-up: *1.* Glass cuvette *2.* Teflon cup *3.* Teflon cap *4.* Electrolyte 0.01–1 *M* KCl, pH 6.2 *5.* Reversible electrodes, Ag/AgCl *6.* Plastic pipe *7.* Ear-phone *8.* Function generator, Textronics FG504 *9.* Current-to-voltage converter, Keithley 427 *10.* Oscilloscope C1–78 *11.* Phase sensitive analyser, PAR 5204 *12.* Switch *13.* D.c. voltage source *14.* Boxcar averager, PAR Model 162 *15. X-Y* recorder

lov (1973). The Teflon cup with a very small internal volume (0.25 cm^3) was closed by a Teflon cap. One of the Ag/AgCl electrodes was mounted in the cap, the second one being immersed in the glass cuvette. Through an opening in the cap connected to a flexible pneumatic pipeline oscillating air pressure was applied over the electrolyte surface and was transferred in this way to the membrane. Air pressure was generated by an electrically shielded ear-phone[1]. The ear-phone was fed by a function generator, FG504 (Textronics). Applied frequency was in the range 10–1,000 Hz. Using a *T*-pipe, an open branch filled with cotton wool was introduced in the pipeline in order to equilibrate any static pressure difference between the two membrane sides but to transfer the dynamic air pressure. The experimental set-up is shown schematically in Fig. 1. After spreading the membrane, its planarity was adjusted by varying the solution level outside the cap and its capacitance was measured. The first important point in the study of the curvature-electric effect was to evaluate the membrane curvature and to assure its constancy at each frequency applied. The membrane curvature was adjusted using the "condenser micro-phone effect" (Ochs and Burton 1974). Namely, a small potential difference (100 mV) was applied to the membrane and the displacement current due to the oscillations of the membrane capacitance was recorded. From the amplitude of the capacitance oscillations the curvature was evaluated.

Assuming that the deformed membrane has the shape of a spherical cap with radius of the sphere, R, and radius of the cap, r (equal to the planar BLM radius) the curvature can be found by simple geometry (Petrov and Derzhanski 1976):

$$c = \frac{1}{R} = \frac{\sqrt{\Delta S/S_0}}{1+(\Delta S/S_0)} \cdot \frac{2}{r}, \tag{2.1}$$

where ΔS is the excess area of the cap-like membrane with respect to the membrane area, S_0. As $\Delta S \ll S_0$ one can safely neglect their ratio in the denominator. Then, from (1.2) and (2.1)

$$S = S_0 + \Delta S = S_0 + \Delta S_m \sin^2 \omega t \tag{2.2}$$

where

$$\Delta S_m = \tfrac{1}{4} S_0 r^2 c_m^2 .$$

Equation (2.2) shows that for *one* period of the curvature oscillation the membrane area twice reaches a maximum. The membrane capacitance will display similar behaviour:

$$C = C_0 + \Delta C_m \sin^2 \omega t . \tag{2.3}$$

In our measurements, $\Delta C_m =$ constant was always maintained at each frequency (see below). However, the relationship between $\Delta C_m/C_0$ and $\Delta S_m/S_0$ is frequency-dependent (Wobschall 1971; Szekely and Morash 1980). In general

$$\frac{\Delta C_m}{C_0} = \frac{\Delta S_m}{S_0} Q(\omega) , \tag{2.4}$$

where the shape of $Q(\omega)$ depends on the correlation between the elastic and viscosity parameters of the torus and BLM. Three limiting regimes of membrane bulging could be recognized in this respect:

Slow bulging: At very low frequencies ($\nu < 0.1$ Hz) a buildup of the BLM takes place by pulling excess area, ΔS, from the torus, with consequent thinning. The BLM thickness remains unchanged. In this limit $Q(\omega) = 1$ and

$$\Delta C_m/C_0 = \Delta S_m/S_0 . \tag{2.4'}$$

Medium bulging: At higher frequencies ($\nu \gtrsim \nu_m \sim 1$ Hz) the stretched portion, ΔS, of the torus has no time to thin down to BLM thickness and makes no contribution to the capacity response. Consequently, the capacitance change must drop because only the stretching of the BLM part will contribute. During

1 Thanks are due to V. I. Passechnik, DSc, Moscow State University, for kindly providing us with the vibrating system

the stretching of an incompressible membrane an equal relative decrease of its thickness must occur, so that the respective capacitance change increases by a factor of two. However, the percentage of the BLM stretching is governed by the ratio, α, of the torus elasticity to the sum of BLM and torus elasticity and under typical conditions (higher temperatures) one has $\alpha \ll 1$. Usually, values of $\alpha \sim 0.05$ are quoted. Now $Q(\omega) = 2\alpha$ and

$$\Delta C_m / C_0 = 2\alpha (\Delta S_m / S_0) . \qquad (2.4'')$$

The medium bulging regime displays a mid-frequency plateau $[\nu_m, \nu_h]$ in the capacitance response. It occurs when the frequency is too high for thinning to occur but not high enough for the torus viscosity to be effective. The high frequency break, ν_h, is in general bigger than 100 Hz and depending on the torus viscosity can reach 1,000 Hz.

Fast bulging: At still higher frequency ($\nu \gg \nu_h$) the torus is not stretched at all and the whole area increase is provided by the BLM, that is $Q(\omega) = 2$ and

$$\Delta C_m / C_0 = 2 (\Delta S_m / S_0) . \qquad (2.4''')$$

With $\Delta\varphi$ applied the charge on the membrane capacitance is $Q = \Delta\varphi C$ and the current is

$$I = \Delta\varphi \dot{C} = \Delta\varphi \Delta C_m \omega \sin 2\omega t . \qquad (2.5)$$

This current is second harmonic with respect to the vibration and its amplitude is

$$I_{2\omega} = \Delta\varphi \Delta C_m \omega . \qquad (2.6)$$

Consequently, a calibration of $I_{2\omega}$ in such a way that it grows linearly with the frequency will assure a constant value of ΔC_m. The desired value of $I_{2\omega}$ was adjusted by varying the amplitude of the driving signal, i.e. considering the air as incompressible, by varying the peak volume of electrolyte enclosed in the spherical cap-like membrane. Calculation of the membrane curvature from ΔC_m requires, as we have seen, an elucidation of the actual bulging regime. Complete study of the capacity response down to very low frequency was not performed in this work because the vibrating system was not suitable for this purpose and the "condenser microphone effect" employed had very low sensitivity in this range. Consequently, the ratio α was not experimentally determined so that the curvature could only be estimated. The lower limit of our frequency range (10–20 Hz) is safely within the range of the medium bulging regime. The higher limit of 900 Hz – 1,000 Hz may be out of this range depending on the torus viscosity, which is also unknown. If so, however, a gradual reduction of the driving signal necessary to keep ΔC_m = constant should be observed, while experimentally an increase was actually found. Therefore we believe that all the data up to at least 400–500 Hz were within the medium bulging regime. In that case the constant curvature maintained is

$$c_m = \sqrt{\frac{\Delta C_m}{2\alpha C_0}} \cdot \frac{2}{r} . \qquad (2.7)$$

Membrane currents, $I_{2\omega}$ and I_ω, were first amplified by a current-to-voltage converter, Keithley 427, and then analyzed by a lock-in analyzer Model 5204 (Princeton Applied Research) under a regime of second harmonic $I_{2\omega}$ (when $\Delta\varphi = 100$ mV) and first harmonic I_ω (when $\Delta\varphi = 0$) measurement. The lock-in analyzer was synchronized by the driving signal from the function generator and the phases of both signals, $\varphi_{2\omega}$ and φ_ω, were measured with respect to the driving signal. After that the relative phase of the curvature-electric signal with respect to the curvature oscillation of the membrane itself was calculated according to

$$\varphi_0 = \varphi_\omega - \tfrac{1}{2}\varphi_{2\omega} , \qquad (2.8)$$

where the multiplier (1/2) expresses the fact that the capacitance current phase changes *two* times from 0° to 360° for *one* cycle of the driving signal.

In our experiments, $\Delta\varphi = 100$ mV was applied and with an amplification ratio of the Keithley 427, $\varkappa = 10^7$ V/A, the root mean square value of the second harmonic was adjusted according to

$$U_{2\nu}^{\mathrm{RMS}}[\mathrm{V}] = (1/\sqrt{2})\, \varkappa I_{2\nu}[\mathrm{A}] = 10^{-5} \nu [\mathrm{Hz}] .$$

Such calibration corresponds to

$$\Delta C_m = \frac{I_{2\nu}}{\Delta\varphi \cdot 2\pi\nu} = \frac{10^{-5} \cdot \sqrt{2}}{10^7 \cdot 0.1 \cdot 2\pi} = 2.25 \text{ pF} . \qquad (2.9)$$

Separate capacitance measurements yield for the thickness of PE/n-decane membrane, $d = 4.2$ nm. With a typical value of the membrane capacitance, $C_0 = 2.5$ nF, the planar capacitor expression (1.10) gives

$$r = \sqrt{\frac{C_0 d}{\pi \varepsilon \varepsilon_0}} = 0.43 \text{ mm} . \qquad (2.10)$$

Then, the radius of curvature, $R_m = 1/c_m$, according to (2.7) with $2\alpha \sim 0.1$ (medium bulging regime) is

$$R_m = \sqrt{\frac{0.1 \times 2{,}500}{2.25}} \times \frac{0.43}{2} = 2.3 \text{ mm} .$$

Although the BLM radius (and capacitance) vary from membrane to membrane, depending on the size of the torus, these variations do not directly affect the final value of the flexo-coefficient which can be calculated from any individual measurement provided the same calibration of ΔC_m is done with each membrane. Indeed, with r from (2.10), the ex-

pressions (2.6) and (2.7) show that c_m is proportional to C_0^{-1} i.e. C_0 in fact drops out from the flexoelectric current expression, (1.9). There is, however, an indirect influence: a smaller torus results in a smaller α ratio (Wobschall 1971). Fortunately, the $\sqrt{\alpha}$ dependence is not very pronounced.

Surface potentials of the BLM were measured separately in a two chamber Teflon cell by using the same buffer and membrane forming solution. In these measurements, the inner membrane field compensation method, under an ionic strength gradient, was employed (Sokolov 1982; Cherny et al. 1980). Briefly, non-zero surface charge under an ionic strength gradient resulted in a surface potential difference. To get this ionic strength gradient a small amount of concentrated KCl was added to one of the chambers. A sinusoidal voltage was applied to the membrane. In this case a second harmonic signal could be separated from the capacitance current, modulated by the membrane electrostriction, if the inner membrane field was non-zero. To compensate for the second harmonic, and hence for the inner membrane field, it was necessary to apply a voltage bias. The value of the voltage bias nullifying the second harmonic was equal to the BLM surface potential difference. A set-up for automatic compensation developed earlier (Cherny et al. 1980) was applied. The surface charges were calculated from surface potential differences by using simple Gouy-Chapman relationships.

3. Theory

As we have mentioned in the Introduction the curvature-electric polarization per unit area of the membrane is given by a simple linear relationship:

$$P_s = f(c_1 + c_2)\,. \tag{3.1}$$

The vectorial character of the polarization is consistent with the vectorial symmetry of a curved membrane. The convention about the sign of the flexoelectric coefficient, f, attributes a positive sign to it when the polarization points outwards from the centre of curvature of the membrane surface. A molecular basis of the flexoelectricity of lipid bilayers is provided by the asymmetric redistribution of charges (C) and dipoles (D) of the lipid molecules and the splayed uniaxial orientation of their quadrupoles (Q) as a result of the curvature. In general

$$f = f^C + f^D + f^Q\,. \tag{3.2}$$

3.1 Blocked lateral lipid exchange (Fig. 2)

3.1.1 Dipole contribution. In the case of an oscillating BLM two limiting regimes are of importance with respect to the charge and dipole contribution: free lateral lipid exchange with the torus and blocked lateral lipid exchange. With blocked exchange realized in the high frequency limit the outer monolayer of the curved membrane is expanded and the inner one is compressed with respect to the midsurface, the difference being most pronounced in the region of polar heads. Consequently, the theory gives for the dipole contribution (Petrov and Pavloff 1979; Petrov 1984):

$$f^{DB} = -\left(\frac{\mathrm{d}\mu}{\mathrm{d}A}\right)_{A_0} \cdot d\,, \tag{3.3}$$

where $\mathrm{d}\mu/\mathrm{d}A$ is the area derivative of the normal component of the dipole moment μ per molecule, taken at A_0, the area per lipid over the mid-surface. The origin of the area dependence of μ was discussed earlier.

3.1.2 Charge contribution. In discussing the charge contribution to the flexoelectric polarization, $P_s = f^C(c_1 + c_2)$, one should have in mind that the dipolar moment of a system of charges with non-zero total charge has no absolute meaning and depends on the position of the origin of the coordinate system. Here we will take as a natural coordinate plane the mid-plane of the BLM. Such a definition results in an expression for the displacement current (1.5) which coincides with its direct calculation (see below).

Let there be a non-zero partial charge, β, per head group ($\beta \gtrless 0$) over the two membrane surfaces, so that the surface charge density is $\sigma_s = \beta e/A$, where e is the proton charge. Further, let the value of β be able to vary with the area stretching/compressing[2].

The charge contribution to the blocked flexocoefficient, f^{CB}, can be calculated according to the following relationships:

$$\begin{aligned} P_s &= e\left(\frac{\beta}{A_0} + \frac{\mathrm{d}\beta}{\mathrm{d}A}\cdot\frac{\Delta A^o}{A_0}\right)\frac{d}{2} - e\left(\frac{\beta}{A_0} + \frac{\mathrm{d}\beta}{\mathrm{d}A}\cdot\frac{\Delta A^i}{A_0}\right)\frac{d}{2} \\ &= e\left(\frac{\mathrm{d}\beta}{\mathrm{d}A}\right)_{A_0}\cdot\frac{d}{2}\,\frac{\Delta A^o - \Delta A^i}{A_0} \\ &= e\left(\frac{\mathrm{d}\beta}{\mathrm{d}A}\right)\cdot\frac{d}{2}\cdot d(c_1 + c_2)\,; \end{aligned} \tag{3.4}$$

2 Possible reasons for a non-zero derivative ($\mathrm{d}\beta/\mathrm{d}A$) could be some changes in the adsorption/desorption of counter ions and shift of the proton equilibrium over the membrane surfaces in connection with the packing-induced changes of the lipid polar head conformation. Such conformational changes will change the accessibility of the charged groups for protons and counter-ions. With respect to protons this could be expressed in terms of a bending-induced shift of the surface pK values of the ionizable groups over the membrane surface. Thanks are due to Dr. I. G. Abidor and Dr. V. F. Pastushenko for clarifying discussions on this point

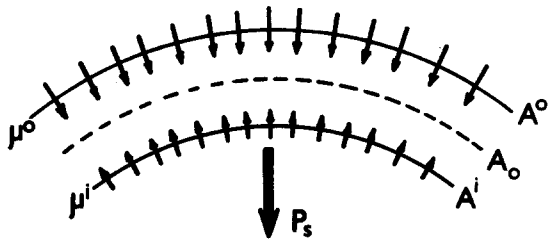

Fig. 2. Flexoelectric polarization of a bent membrane for blocked lipid exchange. A_0 – area per lipid with respect to the midsurface, A^o – area per lipid over the outer (expanded) membrane surface, A^i – area per lipid over the inner (compressed) membrane surface, μ^o (μ^i) – dipole moment per lipid heat at the outer (inner) surface

where $\Delta A^o/A_0$ (or $\Delta A^i/A_0$) is the relative expansion (or contraction) of the area per molecule over the outer (inner) membrane surface. Consequently,

$$f^{CB} = \frac{e}{2}\left(\frac{\mathrm{d}\beta}{\mathrm{d}A}\right)_{A_0} \cdot d^2. \tag{3.5}$$

If the actual situation corresponds to the adsorption of more charges (increase of β) when stretching the interface, the sign of f^{CB} should be equal to that of σ_s.

Direct calculation of the displacement current which will arise in the blocked lateral exchange case with $\frac{\mathrm{d}\beta}{\mathrm{d}A} \neq 0$ can be done by realizing that the charge decrease over the inner membrane surface

$$\Delta Q = S_0 e\left(\frac{\mathrm{d}\beta}{\mathrm{d}A}\right)_{A_0} \cdot \frac{\Delta A^i}{A_0}$$

$$= S_0 e\left(\frac{\mathrm{d}\beta}{\mathrm{d}A}\right)_{A_0} \cdot \frac{d}{2} 2\, c_m \sin \omega t \tag{3.6}$$

will appear as a charge increase over the outer one, or vice versa. Then the current is simply $I = d(\Delta Q)/\mathrm{d}t$, so that

$$I_\omega = S_0 e \left.\frac{\mathrm{d}\beta}{\mathrm{d}A}\right|_{A_0} \cdot d\,\omega\, c_m. \tag{3.7}$$

Just the same result can be got by substituting f^{CB} of (3.5) into (1.5).

3.1.3 Quadrupole contribution. The quadrupolar coefficient, f^Q, does not depend on the lateral exchange rate. As shown previously (Petrov 1984) it is given by

$$f^Q = -\tfrac{1}{3}(L_{zz} - \tfrac{2}{3})\frac{2}{A_0}\Theta_a^M \bar{S}, \tag{3.8}$$

where $L_{zz} \gtrsim 1$ is the $z\,z$ component of the Lorentz local field tensor, $2/A_0$ is the number of lipids per unit area (in both monolayers),

$$\Theta_a^M = \Theta_{zz}^M - \tfrac{1}{2}(\Theta_{xx}^M + \Theta_{yy}^M)$$

is the anisotropy of the molecular quadrupolar moment tensor, and $\bar{S}$ is the mean degree of uniaxial molecular order.

We see that the three components of f have a different power dependence on the membrane thickness, which could be utilized to discriminate between them:

$$f^{CB} \sim d^2; \quad f^{DB} \sim d^1; \quad f^{QB} \sim d^0. \tag{3.9}$$

Both f^D and f^Q are negative, while the sign of f^C depends on the sign of σ_s.

3.2 Free lateral lipid exchange (Fig. 3)

Let us now consider the case of free lateral exchange (low frequency limit) when there is enough time for the lipid molecules to go to the torus from the inner monolayer of the curved membrane, in order to diminish the elastic strains due to its compression, or to come from the torus to the outer monolayer because of its stretching. In such a case, from the point of view of the curvature elasticity theory, the bending of a bilayer is equivalent to the bending of two uncoupled monolayers, each of them having its own neutral surface at a distance δ_N from the mid-surface (Petrov and Bivas 1984). δ_N depends on the distribution of the lateral pressure across each monolayer (Petrov and Bivas 1984). In general $\delta_N < \frac{d}{2}$. The number of lipids per unit area over the neutral surface is equal to that in the flat state. This means, however, that with respect to the

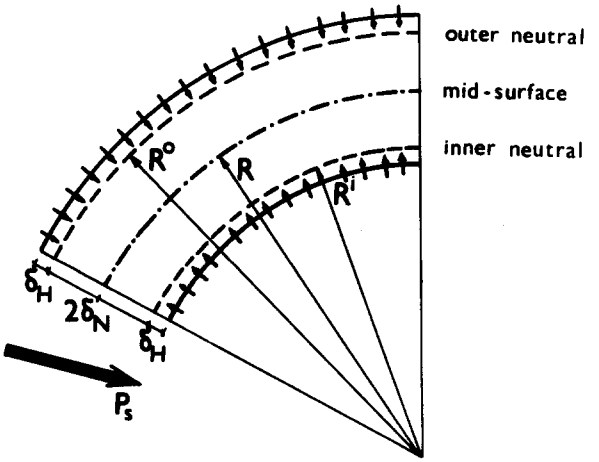

Fig. 3. Flexoelectric polarization of a bent membrane for free lipid exchange. δ_N – distance between the neutral surface and the mid-surface, δ_H – distance between the neutral surface and the head surface

midsurface there will be more charges and dipoles in the outer monolayer than in the inner one.

3.2.1 Dipole contribution. In the calculation of the dipole contribution one also takes into account the fact that the neutral surfaces are nearer to the midplane than the membrane interfaces where the dipoles, μ, are located, so that a residual compression/stretching in these regions also requires a contribution from the blocked mechanism (Petrov 1984):

$$f^{DF} = -2\left(\frac{\mu}{A_0}\right)\delta_N - 2\left(\frac{\mathrm{d}\mu}{\mathrm{d}A}\right)_{A_0}\delta_H, \tag{3.10}$$

where $\delta_H = \frac{d}{2} - \delta_N > 0$. The signs of both terms in (3.10) explicitly take into account the usual dipolar direction towards the hydrophobic bilayer core, leading to $f^{DF} < 0$, also.

3.2.2 Charge contribution. Analogous considerations can be made for the case of a charged membrane. Calculating the polarization one should pay attention to the fact that equalization of the number density of molecules is taking place with respect to the neutral surfaces, while the charges are located over the membrane interfaces. The result for f^{CF} is:

$$f^{CF} = e\left(\frac{\beta}{A_0}\delta_N + \left(\frac{\mathrm{d}\beta}{\mathrm{d}A}\right)_{A_0}\delta_H\right)\cdot d. \tag{3.11}$$

The first contribution to f^{CF} has the sign of σ_s, while the sign of the second should be determined from the experimental data on monolayers (see below).

3.2.3 Quadrupole contribution. This contribution should be identical blocked lateral exchange case (Eq. 3.8).

3.2.4 Displacement current in the low frequency limit. Let us derive an expression for the current in the low frequency limit. Now the assumption (1.3) is no longer valid. If a curvature, $c_1 + c_2$, is created instantaneously, the curvature-induced polarization, P_s, tends to its saturated value, P_s^m, (1.1) with a relaxation time τ, obeying, at any time, the differential equation

$$\frac{\mathrm{d}P_s}{\mathrm{d}t} = \frac{1}{\tau}(P_s^m - P_s). \tag{3.12}$$

With curvature oscillating like (1.2) the saturated polarization will also oscillate:

$$P_s^m = f^F \cdot 2\, c_m \sin\omega t. \tag{3.13}$$

Putting (3.13) into (3.12) we get the steady-state solution

$$P_s(t) = \frac{2 f^F c_m}{\sqrt{1+\omega^2\tau^2}}\sin(\omega t - \varphi), \tag{3.14}$$

where $\mathrm{tg}\,\varphi = \omega\tau$. Now the current according to (1.5) will be

$$I^F = 2 f^F \frac{S}{d} c_m \frac{\omega}{\sqrt{1+\omega^2\tau^2}}\cos(\omega t - \varphi). \tag{3.15}$$

If we compare this expression with the corresponding one for blocked exchange (1.5):

$$I^B = 2 f^B \frac{S}{d} c_m \omega \cos\omega t \tag{3.16}$$

we see that the I^B amplitude increases linearly with the frequency, while that of I^F, after initial growth, tends to a saturated value, $2 f^F (S/d)(c_m/\tau)$ when $\omega > \tau^{-1}$. The phase shift of I^F with respect to the curvature oscillation (1.2) changes from $-\pi/2$ to 0 on increasing the frequency, while I^B is permanently shifted to $-\pi/2$ (or $+3\pi/2$). In the transition region from the low frequency to the high frequency regime some interference between the two mechanisms of curvature polarization is possible so that the current could deviate from the simple sum of I^F and I^B.

4. Results

Some recordings of the curvature-electric signals and "condenser microphone" signals are shown in Fig. 4a, b, c. They were recorded by a Boxcar Averager, Model 162 (EG & G Princeton Applied Research) and demonstrate the doubled frequency of the capacitance signal, the basic frequency of the curvature-electric one, and the phase shift between them. The capacitance signal was always recorded with a 100 mV constant potential difference across the BLM.

Figure 4a also demonstrates the amplitude dependence of the curvature-electric signal when increasing amplitudes of the mechanical stimulus were applied. The lowest one corresponds to the calibrated curvature (i.e. calibrated amplitude of the second harmonic) as described in Sect. 2. It can be seen that at higher amplitudes a second harmonic component of the curvature-electric signal is also generated. This may be explained by the more complicated non-spherical shape of the vibrating membrane, i.e. by the excitation of overtones at increased pressure difference (Passechnik and Sokolov 1975).

Figure 4b gives an idea about the frequency dependence of the electric signal amplitude at two

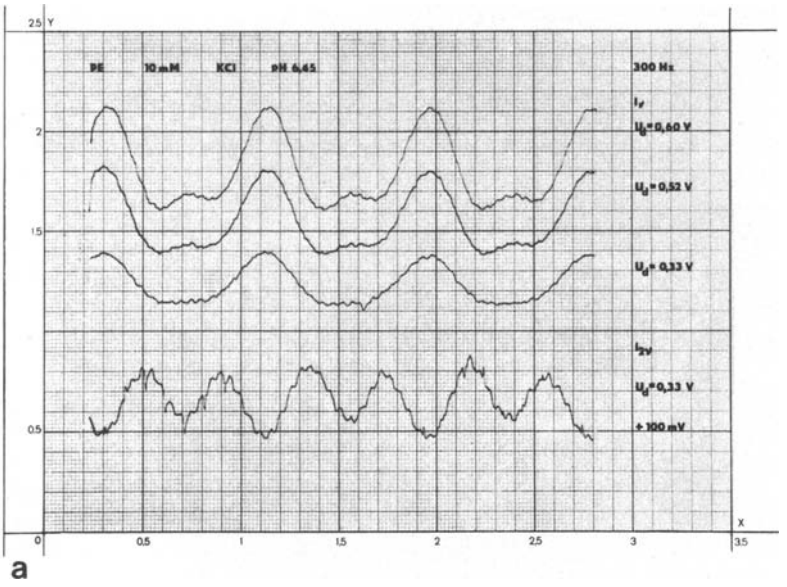

Fig. 4a. Amplitude dependence of the curvature-electrical signal. I_{2v} – second harmonic, generated by the "condenser microphone effect" with 100 mV externally applied to the membrane, I_v – first harmonic, generated by the membrane itself under short circuit conditions, U_d – RMS value of the driving signal of the earphone. $U_d = 0.33$ V corresponds to the calibrated amplitude of the second harmonic, I_{2v}. The signals are averaged by the Boxcar averager over a time interval of 1 min

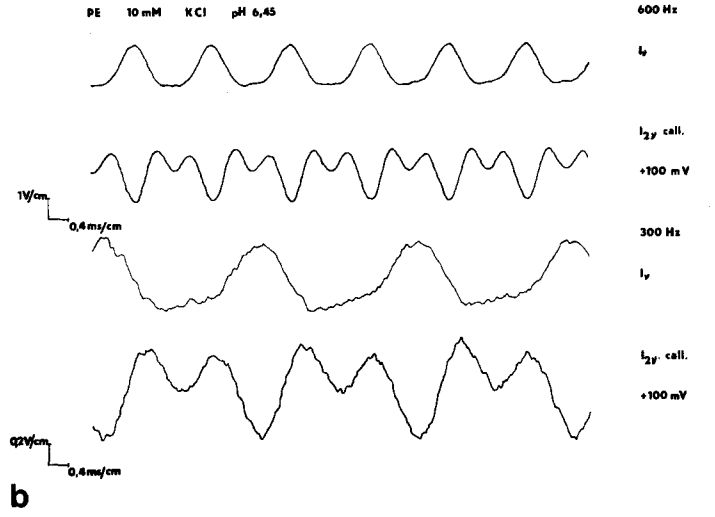

b. Frequency dependence of the curvature-electric signal. The vertical scale of the 300 Hz record is 5 times expanded compared to the 600 Hz. With both records, I_{2v} is calibrated according to Eq. (2.9) of the text to assure the same curvature amplitude

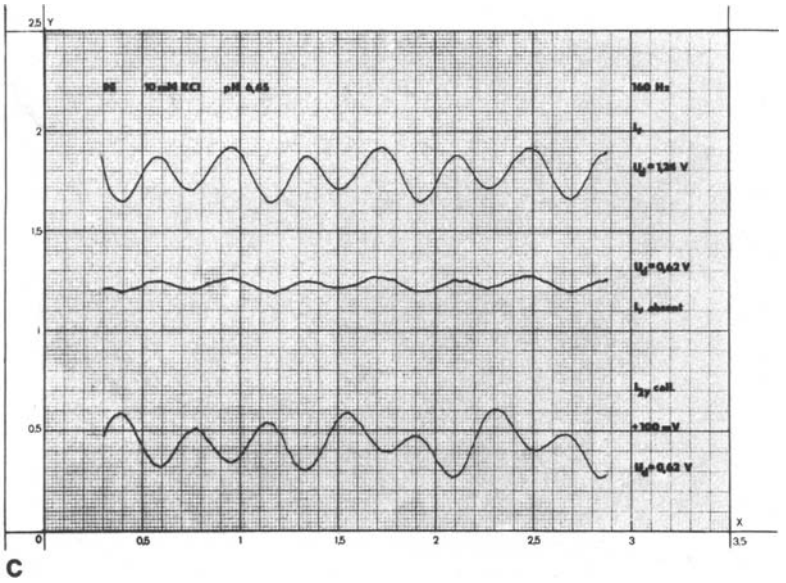

c. Absence of first harmonic I_v in the curvature electric signal at the marginal frequency of 160 Hz. $U_d = 0.62$ V – calibrated curvature amplitude, $U_d = 1.24$ V – elevated curvature amplitude. The first harmonic component (also measured by the lock-in amplifier) is negligibly low. Note the appearance of static membrane curvature by the end of the I_{2v} scan (demonstrated as a disbalance of the "condenser microphone" signal)

frequencies (300 Hz and 600 Hz) with the same calibrated amplitude of the curvature. Note that the vertical scale with 300 Hz is 5 times expanded compared to that with 600 Hz so that I_{600} is about 3 times higher than I_{300}.

Fig. 4c shows the behaviour of the curvature-electric signal at 160 Hz, a frequency which seems to be marginal between the low frequency and the high frequency regime. Practically no first harmonic is generated at 160 Hz with this membrane, even with increased curvature amplitude. Only weak second harmonic noise is present.

On the other hand, at higher frequencies the curvature-electric contribution is sufficiently high and it is also visible in the capacitance signal, reflected in the presence of a first harmonic in this case.

In measuring $I_{2\omega}$ it was necessary to make sure that the membrane oscillates around a flat state. This was realized by varying the hydrostatic pressure difference and looking for symmetry in the capacitance signal (see Fig. 4c). Some waxing and waning of the output signal may be due to the hydrodynamic resonances in the chamber as suggested by Ochs and Burton (1974), although the chamber volume was choosen to be very small in order to minimize them. Evidence for resonance behaviour came from the fact that during the calibration of the curvature amplitude, marked drops in the required values of the driving signal were observed around 60 Hz, 230 Hz and 450 Hz. Nevertheless, the use of the membrane itself as a pressure sensor according to the calibration procedure adopted (see Materials and methods) assured the necessary constancy of the curvature.

4.1 *Amplitude vs frequency*

Amplitude-frequency characteristics of the curvature-electric effect for several membranes in 50 m*M* KCl are shown in Fig. 5. The experimental confirmation of the existence of two regions, the low frequency and high frequency regions, is evident. The limit between these two regions is around 150 Hz.

The measurements in the low frequency region start from 10 Hz. Below 10 Hz they are very difficult. A slight increase of the signal with the frequency up to 50 Hz can be seen, followed by a plateau up to 120 Hz and a marked drop with some membranes in the vicinity of 150 Hz.

In the high frequency region a more or less linear growth of the signal is observed (although there is sometimes evidence for a local maximum at about 650 Hz). The upper limit of 1,000 Hz in our

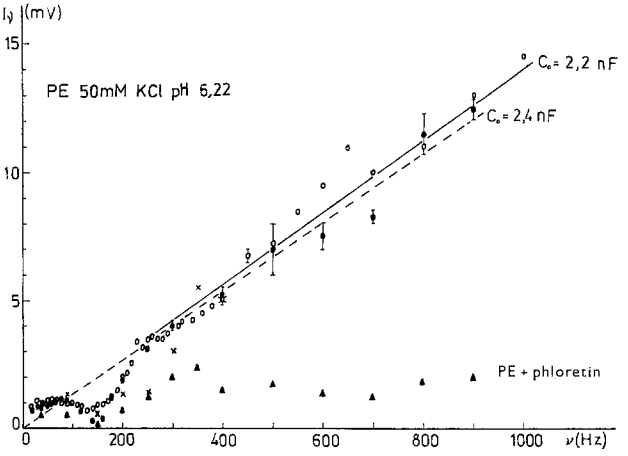

Fig. 5. Frequency dependence of the curvature-electric effect's amplitude. I_ν – RMS value of the first harmonic of the current amplified by Keithley 427 with amplification 10^7 V/A. Bacterial phosphatidyl ethanolamine/n-decane BLM. Electrolyte – unbuffered KCl, 50 m*M*, pH 6.22. ● flat BLM, capacitance $C_0 = 2.4$ nF, ○ $C_0 = 2.2$ nF, × $C_0 = 2.0$ nF, ▲ Phloretin-modified BLM: 40 µl of 10 m*M* phloretin solution in ethanol added to 10 ml bathing electrolyte

experiments comes from the restricted maximal output of the function generator (10 V) which is insufficient to produce the calibrated value of $C_m = 2.25$ pF at higher frequencies. Extrapolation of the high frequency straight line goes approximately to zero. Qualitatively, the shape of the characteristic corresponds to the theory. Quantitative determination of the flexo-coefficients is given below.

4.2 *Phase vs frequency*

In Fig. 6, the frequency dependence of the relative φ_0 of the flexoelectric signal is shown. It is calculated with respect to the phase of the membrane curvature according to (2.8). It is characterized by a low frequency plateau and a high frequency plateau, with a gradual transition between them. In the phase measurements it was necessary to pay attention to the pronounced delay of the phase of the "condenser microphone" signal, $\varphi_{2\omega}$, with respect to the driving signal. In the interval 20–1,000 Hz, $\varphi_{2\omega}$ passed 7 times through 0°, gradually decreasing in a monotonic way. Therefore at lower frequencies it was necessary to measure the phase every 10–20 Hz in order to find all successive points of zero phase and to avoid confusion in the determination of the phase $\varphi_{2\omega}$ in a continuous manner. After assigning a positive sign for the first phase values all phases subsequently passing through 0° were treated as negative, adding after each subsequent point of zero phase another – 360°. In the final result for $\varphi_0 = \varphi_\omega$

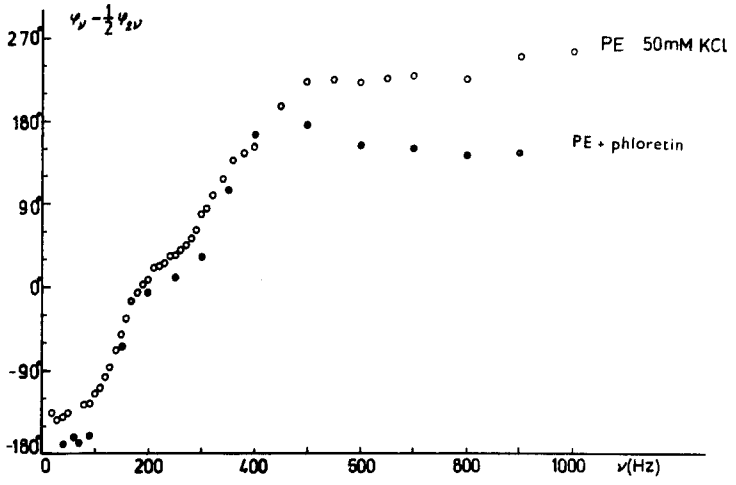

Fig. 6. Frequency dependence of the relative phase of the curvature-electric effect. ○ same BLM as Fig. 5 ($C_0 = 2.2$ nF), ● same phloretin-modified BLM as Fig. 5

Table 1. Measured surface potential differences of a phosphatidyl ethanolamine/n-decane BLM and calculated surface charge and surface potential

Volume of 2.5 *M* KCl added to the front compartment [μl]	4	10	20	40
Surface potential difference U_i [mV]	− 0.7	− 4.9	− 9.6	− 11.7
Surface charge σ_s [μC/cm²]	− 0.4	− 1.2	− 1.4	− 1.2
Surface potential φ_s [mV]	− 8	− 22	− 26	− 23

$-\frac{1}{2}\varphi_{2\omega}$, the high frequency phases were assumed positive and the low frequency phases − negative (i.e. equal to $\varphi_0 - 360°$). The relative phase defined in this way passes through zero in the vicinity of 200 Hz i.e. near (but higher than) the marginal frequency.

4.3 Surface charge determination

Measurements of the surface potential difference, ΔU_i, under an ionic strength gradient, were performed on BLM formed from the same PE/n-decane solution as the membranes from Figs. 5 and 6, and in the same electrolyte (50 m*M* KCl, pH 6.2), in another cell with two identical chambers, each 1 ml in volume. Successive amounts of 2.5 *M* KCl were added to one of the chambers and by the method of inner membrane field compensation (Materials and methods) ΔU_i, and from it σ_s, were calculated. Results from one typical measurement are reported in Table 1.

As the first amount added (4 μl) is very small and errors in the volume are possible the results from it are usually not very reliable. Neglecting them, a mean value of

$$\sigma_s = -1.3 \times 10^{-6}\ \mathrm{C/cm^2}$$

could be derived. Such values, as numerous measurements at this pH showed, were typical for the membranes formed 2−3 days after the preparation of the membrane forming solution, which was stored in a refrigerator during that period. These values reflected the presence of a small percentage of charged impurities ($\beta = 3.7\%$ if the mean area per lipid was assumed to be equal to 45 Å² or 3.7% of the total number of molecules bearing one elementary charge, e^-). This percentage was stable with time, for storage of the membrane forming solution in a closed vial at − 4 °C. Only with very fresh preparations could smaller surface charge densities (of the order of 0.1 μC/cm²) be measured, sometimes of positive sign and quite irreproducible.

4.4 Amplitude vs peak curvature

Figure 7 shows the amplitude characteristic of the curvature-electric effect at two frequencies, one below the marginal frequency (70 Hz) and one above it (400 Hz) are shown. The flexoelectric signal, I_ω (with $\Delta\varphi = 0$) as a function of the square root of the second harmonic $I_{2\omega}$ (with $\Delta\varphi = 100$ mV) is plotted. The $\sqrt{I_{2\omega}}$ is taken as a variable, because the amplitude of the membrane curvature, c_m, is, according to (2.7) and (2.5), proportional to it. Both characteristics are linear down to very small curvatures, as the nature of the curvature electricity requires. Deviations from linearity can be seen only at higher mechanical amplitudes (e.g. at the last three points of the 70 Hz line, overtones were excited). The calibrated values at which the points

on the frequency characteristic (Fig. 5) were measured are shown by double circles. They are well within the linear region.

4.5 *Determination of the sign of the flexo-coefficient*

Phase measurements on initially curved membranes were performed with the aim of determining the sign of the flexoelectric coefficients at the same frequencies of 70 Hz and 400 Hz, as in Fig. 7. In Fig. 8, the scheme of the measurements and the results are reported. Now the membrane oscillates around a curved state and if this static curvature is bigger than the oscillation amplitude, so that the planar state is never reached, the membrane capacity oscillates with the same and not with the doubled frequency:

$$C = C_0 + \Delta C \sin \omega t . \tag{4.1}$$

The membrane polarization now contains a constant term:

$$P = P_0 + \Delta P \sin \omega t . \tag{4.2}$$

The capacitance current density is

$$i_C = \frac{1}{S} \omega \, \Delta\varphi \, \Delta C \cos \omega t \tag{4.3}$$

so that it is now also a first harmonic and its phase depends on the relative sign of ΔC with respect to the sign of the transmembrane voltage. The sign of ΔC is connected to the sign of the static curvature. By a change of this curvature to the opposite one should change the phase of the capacitance current by 180°. Experimentally, the change is 130° ± 40° (Fig. 8a, b and c, d).

The flexoelectric current density is

$$i_P = \frac{d}{dt}\left(\frac{P_s}{d}\right) = \frac{\omega \, \Delta P}{d} \cos \omega t \tag{4.4}$$

and its phase depends on the direction of the curvature-induced polarization with respect to the curvature, i.e. on the sign of the flexoelectric coefficient. By the change of the static curvature to the opposite one should not influence the phase of the flexoelectric current, as observed. Both i_C and i_P are of displacement origin.

The comparison between the i_C and i_P phases is also shown in Fig. 8. As before, the lock-in detector is synchronized by the driving signal so that the absolute values of phases, reflecting the phase shift between the maximal pressure in the vibrator and maximal membrane curvature, are unimportant for our discussion. The capacitance current (with $\Delta\varphi \neq 0$) and the flexoelectric current (with $\Delta\varphi = 0$) should be

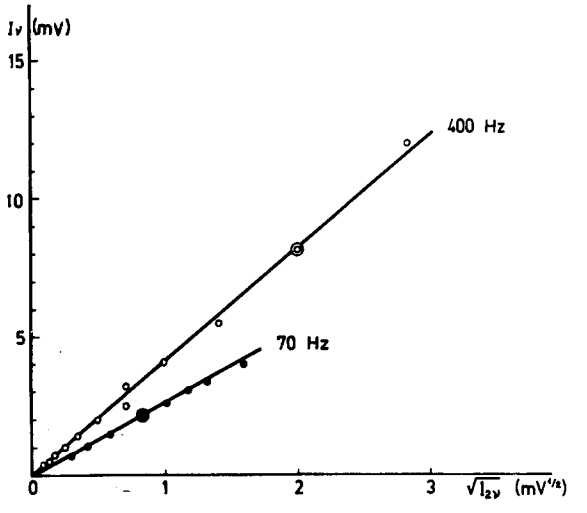

Fig. 7. Amplitude dependence of the curvature-electric effect. Membrane curvature is proportional to $\sqrt{I_{2\nu}}$. ● oscillation frequency $\nu = 70$ Hz (free lipid exchange regime), ○ oscillation frequency $\nu = 400$ Hz (blocked lipid exchange regime). *Doubled circles* – calibrated curvatures employed for the frequency characteristics in Fig. 5 (see Materials and methods)

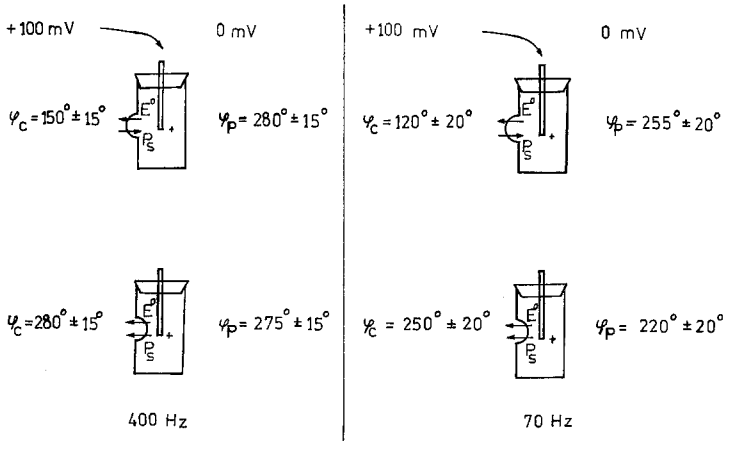

Fig. 8. Determination of the sign of the flexo-coefficient by initially curved membranes at two oscillation frequencies: $\nu = 400$ Hz (blocked lipid exchange regime) and $\nu = 70$ Hz (free lipid exchange regime). φ_C measurements were performed with + 100 mV transmembrane voltage applied to the inner electrode. When φ_C and φ_P coincide the membrane polarization P_s is directed like the transmembrane field, E_0 (see the text). These results show that the flexo-coefficients are negative in both regimes

in-phase when the static curvature-induced polarization is directed in the same way as the transmembrane electric field applied in the capacitance measurements. Only then will the situation of increasing membrane capacitance (i.e. increase of the static membrane curvature) correspond to an increase of the total curvature polarization in the positive direction of the axis defined by the electric field, i.e. ΔC and ΔP will have the same sign (compare (4.3) and (4.4)). For both frequencies this in-phase situation takes place in the case of the inward curved membrane (Fig. 8b and d) and in view of the fact that a positive potential was applied to the electrode inside the closed cup a conclusion can be drawn that the flexoelectric polarization points towards the centre of curvature of the membrane surface. This means that the flexoelectric coefficient has a negative sign both in the low frequency and in the high frequency region. Such a finding is in accord with the theoretically expected sign of the dipolar contribution, f^D, and of the charge contribution, f^C, for a negative surface charge density, as found in our experiments.

In these measurements we noticed that the flexoelectric signal, I_ω at $\Delta\varphi = 0$, was influenced by the value of the static curvature. An increase up to 3 times in 50 mM KCl and up to 10 times in 10 mM KCl was observed for some particular measurements in the course of a continuous variation of the static BLM curvature from zero up to approximately a hemisphere. In part, this effect could be explained as being simply due to the increased membrane area, S_0 (Eq. (1.6)), although some curvature dependence of the flexo-coefficient itself could not be excluded. Indeed, the theory predicts a proportionality of f to the derivatives $\mathrm{d}\mu/\mathrm{d}A$ and $\mathrm{d}\beta/\mathrm{d}A$ (Eqs. (3.3) and (3.5)). Having in mind that in a bent membrane the areas per head over both monolayers are different from the flat state the derivatives might take different values. The marked ionic strength dependence further points to the important role of the charge contribution, $\mathrm{d}\beta/\mathrm{d}A$ (see below).

4.6 *Calculation of the flexo-coefficients*

4.6.1 High frequency limit (blocked lateral exchange). The "blocked" flexo-coefficient, f^B, can be calculated from the peak value of the flexoelectric current at a given frequency, I_ν, by means of Eq. (1.9). Expressing C_0 from (1.10) and c_m from (2.7) the final expression for f^B is:

$$f^B = \frac{I_\nu}{8\pi\nu}\sqrt{\frac{2\alpha\varepsilon\varepsilon_0 d}{\pi\Delta C_m}}\,, \tag{4.5}$$

where ΔC_m is the calibrated amplitude of the capacitance change of the oscillating membrane. As we mentioned before, f^B is independent of C_0.

The peak current is given by $I_\nu[\mathrm{A}] = \sqrt{2}\,U_\nu[\mathrm{V}]/10^7$, where U_ν is the RMS value of the voltage-converted flexo-signal. With $\nu = 1{,}000$ Hz, $U_\nu = 14$ mV (Fig. 5), $2\alpha \sim 0.1$, $\varepsilon = 2$, $\varepsilon_0 = 8.85$ pF/m, $d = 4.2$ nm and $\Delta C_m = 2.25$ pF (2.9), Eq. (4.5) gives

$$f^B = 25.5\times10^{-19}\,C \quad \text{for PE/n-decane BLM in 50 m}M\text{ KCl, pH 6.2.} \tag{4.6}$$

The relative error of f^B is

$$\frac{\Delta f}{f} = \frac{\Delta I_\nu}{I_\nu} + \frac{1}{2}\left(\frac{\Delta\alpha}{\alpha} + \frac{\Delta d}{d} + \frac{\Delta I_{2\nu}}{I_{2\nu}}\right)$$
$$= 10\% + \tfrac{1}{2}(100\% + 10\% + 5\%) = 72.5\% \tag{4.7}$$

as the relative error of ΔC_m (2.9) is equal to the relative error of the capacitance current adjustment. This large error in f^B comes from the rough estimate for the value of α, the relative error in α is, therefore, taken as high as 100%.

4.6.2 Low frequency limit (free lateral exchange). If the vibrational frequeny is in the region of initial linear growth of the signal, i.e. $(\omega\tau)^2 \ll 1$, the denominator of (3.15) can be neglected and the formula of Eq. (4.5) can be applied for the f^F calculation. Unfortunately, the low sensitivity in this limit gave no possibility for reliable measurements with frequencies sufficiently close to zero, so that the linear region is not well enough revealed and the relaxation time could only be roughly estimated from the plateau position as $\tau \sim 10^{-2}$ s. If, solely for estimation purposes we apply Eq. (4.5) with $\nu = 20$ Hz, $U_\nu = 0.8$ mV and the rest of data as for f^B, we get $f^F = 73\times10^{-19}\,C$. Calculations from the saturated plateau value of the signal, I_∞ for $(\omega\tau)^2 \gg 1$, can be done using a formula which follows from (3.15):

$$f^F = \tfrac{1}{4} I_\infty \tau \sqrt{\frac{2\alpha\varepsilon\varepsilon_0 d}{\pi\Delta C_m}}\,. \tag{4.8}$$

With $\tau \sim 10^{-2}$ s and $U_\infty = 1$ mV this gives

$$f^F = 115\times10^{-19}\,C \quad \text{for PE/n-decane BLM in 50 m}M\text{ KCl, pH 6.2.} \tag{4.9}$$

The relative error of f^F could be as high as 80% considering the higher inaccuracy of I_ν in this region.

For more accurate calculations of f^B and f^F, knowledge of α is necessary, this requires studies of the capacitance response of each particular membrane under investigation down to frequencies of 10^{-2} Hz (Wobschall 1971). However, this could be a long procedure and membrane lifetime problems may prevent one from realizing it. Let us note that a complete run of the frequency characteristic of the flexo-signal from 10 to 1,000 Hz (45–50 points)

takes more than 2 h and only few of the numerous membranes studied were able to last up to the end of the experiment without rupture under such prolonged mechanical excitation.

4.7 Nonactin treatment and influence of the membrane defects

To check the nature of the generated current, BLM were treated with the ionic carrier nonactin. A particular experiment was carried out with the *same* membrane whose frequency characteristic is reported in Fig. 9 (50 mM KCl). Initial membrane conductivity was rather low (estimated value $10^{-10}-10^{-11}\,\Omega^{-1}$). Two subsequent additions of nonactin (dissolved in ethanol) to the outside electrolyte solution (10 ml in volume) were made: 20 µl of $10^{-4}\,M$ nonactin solution and 20 µl of $10^{-3}\,M$ nonactin solution. After the second addition the frequency characteristic of the modified membrane (conductivity increased up to $2\times10^{-8}\,\Omega^{-1}$) was studied in the range 70–400 Hz and was found to be, within the scattering limits, the same as that of the initially unmodified membrane.

These findings could be considered as a proof that the generated current is not of conductive origin but has a displacement character.

The role of defects was demonstrated by a few observations of the signal behaviour just before the membrane rupture. It is known (Chizmadzhev et al. 1982) that before rupturing a BLM is for a limited time in the so-called stress state, characterized by the presence of fluctuating conductivity defects, due to pores in it. In this state a marked increase of the generation current was noticed. In one experiment at 500 Hz the signal increased from 10 mV to more than 25 mV and then the BLM ruptured. This could be interpreted as a change of the flexo-mechanism from blocked to free flip-flop, as the presence of pores with hydrophilic edges is known to increase the flip-flop rate (Taupin et al. 1975). In such a case the effect should increase, indeed, because the flexo-coefficient, f^F, seems to be several times higher than the blocked one, f^B (see above).

4.8 Influence of phloretin

The dipolar modifier phloretin, known to decrease the surface potential of lipid head group dipoles by a value of approximately 100 mV (Andersen et al. 1976; Sokolov et al. 1984) because of its oppositely directed dipolar moment, was used as a $10^{-2}\,M$ solution in ethanol. Upon non-symmetrical addition to the outer side only, of a BLM with normal flexoelectric characteristic in a quantity of 40 µl (in 10 ml bathing electrolyte), it produced no definite effect on the value of the first harmonic U_v, but led to the appearance of a second harmonic, U_{2v}. Simultaneous measurements of the intramembrane field by the compensation method of Cherny et al. (1980) revealed a surface potential of − 50 mV as due to the unilateral adsorption of phloretin. So, the appearance of the second harmonic can simply be explained as a "condenser microphone" effect from an asymmetrical membrane.

Under symmetrical conditions (careful mixing of the inside and outside volumes) the frequency dependence of the amplitude and phase of I_v were studied and were shown in Figs. 5 and 6. The amplitude characteristic demonstrated a drastic drop of the signal in the high frequency region. Moreover, the typical high-frequency linear increase was totally abolished. The signal remained at a more or less constant level. The phase characteristic was not substantially changed. Only the high-frequency plateau was reduced by approximately 90°.

This finding could be considered as a demonstration of the important role of the dipolar flexo-contribution. But as the separate estimations of this contribution, from monolayer data, showed its smallness (see Discussion) another interpretation has to be found.

4.9 Influence of surface charge variation

Attempts to vary surface charge of PE were done by pH variation. Surprisingly, good buffering capacity of PE was found and the largest surface charge deviation induced in this way was $\sigma_s = +1.6\,\mu C/cm^2$ (KH_2PO_4 buffer, pH 3.0). The effect of pH was studied in the low frequency region.

Compared to other pH values, giving surface charge densities from − 1.25 to + 0.9 µC/cm^2 and low frequency plateaus of 1–2 mV, the pH 3.0 buffer gave a plateau value of 4 mV.

The effect of CTAB adsorption was studied in the high frequency region. 20 µl of $10^{-3}\,M$ water solution of this cationic detergent added in 10 ml bathing electrolyte resulted in a 20–40% increase of the signal.

4.10 Ionic strength influence

Electrolyte solutions of non-buffered KCl 10 mM, 50 mM and 1 M were employed. The results are shown in Fig. 9. In the low frequency region the only noticeable influence was upon the limitting frequency, which seemed to increase with decreasing ionic

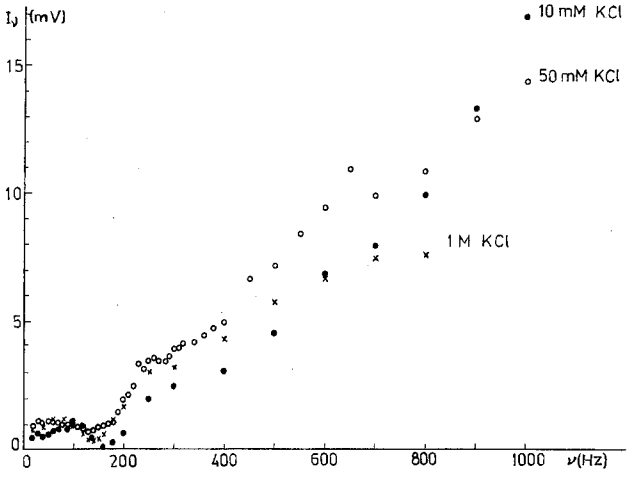

Fig. 9. Influence of the ionic strength on the curvature-electric signal. ● 10 m*M* KCl, ○ 50 m*M* KCl, × 1 *M* KCl

strength. In the high frequency region a marked correlation between the slope of the frequency characteristic and the reciprocal ionic strength was found: from being the lowest at lower frequencies the signal with 10 m*M* electrolyte had the highest frequency increment and in the region of 1,000 Hz was the highest in absolute value. Actually, its frequency dependence was non-linear. Non-linear features could also be seen in the recording in Fig. 4, made with the membrane whose frequency characteristics (10 m*M*) were displayed in Fig. 9. For comparison, the slope of the 1 *M* solution was the lowest and the generated signals were strictly sinusoidal. One should also note the longer term stability of membranes at low ionic strength compared to high ionic strength.

These findings are indicative of the decisive surface charge contribution to the effect under investigation (see below).

5. Discussion

5.1 Theoretical estimations of the flexo-coefficients

Estimation were done on the basis of the theoretical formulae (3.3), (3.5), (3.10) and (3.11). It was shown earlier that the quadrupoles make, in general, a small contribution to the flexoelectricity of lipids, approximately $-0.5 \times 10^{-20}\,C$ (Petrov 1984). The dipolar and charge contributions were evaluated using the data about surface potential *vs* area dependence of monolayers of synthetic 1,2-dipalmitoyl-DL-phosphatidylethanolamine at the air/water interface at different pH and ionic strength values of Standish and Pethica (1968). Although these data were obtained with NaCl electrolyte and no direct correspondence between the partial charge per head and the impurity level could be done, the estimations gave a clear idea about the order of magnitude of the different contributions.

5.1.1 Blocked lateral exchange. The dipolar moment of PE was calculated from the surface potential *vs* area curve $\Delta\varphi(A)$ at pH 7.4 and 0.1 *M* NaCl (corresponding to a zero total charge of the PE zwitterionic head) according to the formula

$$\mu = \varepsilon_0 A \Delta\varphi(A), \tag{5.1}$$

and ranged from $2.15 \times 10^{-30}\,C \cdot m$ at 42 Å^2/mol to $2.34 \times 10^{-30}\,C \cdot m$ at 49 Å^2/mol. Subsequently, $\mathrm{d}\mu/\mathrm{d}A$ values were calculated and, taking $d = 4.2$ nm, f^{DB} values were obtained from (3.3) in the range $-0.16 \times 10^{-19}\,C$ to $-0.04 \times 10^{-19}\,C$, i.e.

$$f^{DB} \sim -0.1 \times 10^{-19}\,C \tag{5.2}$$

a value that *decreases* upon increasing the area per molecule.

f^{CB} was calculated from the $\Delta\varphi(A)$ curve for pH 9.9; 0.1 *M* NaCl. Partial charge per head, β, was calculated according to the Gouy-Chapman relationship for a monovalent electrolyte:

$$\beta = A c^{1/2} \frac{1}{e} \sqrt{8\,\varepsilon_w\,\varepsilon_0 RT}\; s\,h\left(\frac{F\varphi_s}{2RT}\right), \tag{5.3}$$

where R is the gas constant, F is the Faraday number, ε_w is the water dielectric constant and c is the ionic concentration. φ_s is the part of the total surface potential due to the partially charged head groups and was calculated from

$$\varphi_s = \Delta\varphi - \Delta\varphi_d, \tag{5.4}$$

where $\Delta\varphi_d$ is the dipolar potential equal to the surface potential at the isoelectric point, pH 7.4 (see above). Values for β ranged from -2.0% to -3.75% with A in the range 43 Å^2/mol to 49 Å^2/mol, so that f^{CB} ranging from $-2.7 \times 10^{-19}\,C$ to $-7.5 \times 10^{-19}\,C$ was obtained from the numerically calculated $\mathrm{d}\beta/\mathrm{d}A$. One can see that the order of magnitude of f^{CB} is

$$f^{CB} \sim -10 \times 10^{-19}\,C \tag{5.5}$$

and that it *increases* with increasing the area per molecule. The conclusion to be drawn is that in the blocked flip-flop case the contribution from the bending-induced shift of the surface charge equilibrium is 2 orders of magnitude bigger than the dipolar contribution. Further evidence comes from the monolayer data: with decreasing ionic strength the $\Delta\varphi(A)$ curves become steeper, so that an enhancement of f^{CB} could be expected.

5.1.2 Free lateral exchange. If the lateral pressure is homogeneously distributed along the monolayer thickness then $\delta_N = \delta_H = d/4$ (Petrov and Bivas 1984). Considering this case for estimation purposes we get from (3.10)

$$f^{DF} \sim -0.2 \times 10^{-19}\, C \tag{5.6}$$

i.e. the same low order of magnitude as f^{DB}.

The first term of the charge contribution (3.11)

$$(e\,\beta/A)\,\delta_N\, d = \sigma_s\, d^2/4$$

is directly calculatable from the measured surface charge density $\sigma_s = -1.3 \times 10^{-6}\, C/\mathrm{cm}^2$ and $d = 4.2$ nm to be $-0.6 \times 10^{-19}\, C$, while the second one

$$e\,(\mathrm{d}\beta/\mathrm{d}A)\,\delta_H\, d = e\,(\mathrm{d}\beta/\mathrm{d}A)\,(d^2/4)$$

would be one half of the f^{CB} estimated above. So, we get

$$f^{CF} \sim -5 \times 10^{-19}\, C. \tag{5.7}$$

We see that in both blocked and free cases the most important contribution comes from the bending-induced shift of the surface charge equilibrium and that at the measured surface charge density the free exchange charge contribution is only several times higher than that of the dipoles.

5.2 Comparison with the experiment

The theoretically estimated value of f^{CB} (5.5) is in a good agreement with the experimental results for f^B (4.6) from the high frequency region, within the error limits. The agreement between f^{CF} (5.7) and f^F (4.9) is less satisfactory. One reason for higher experimental values could be the larger area per lipid head in a PE bilayer (Shipley (1973): $A_0 = 60$ Å^2; Lis et al. (1982): $A_0 = 74.7$ Å^2) than the available monolayer data used for the estimations above ($A_0 = 40 - 50$ Å^2). As we have seen the data available demonstrated a steep increase of $\mathrm{d}\beta/\mathrm{d}A$ and f^B with the area per head.

A still unresolved problem is the experimental finding that $f^F > f^B$, while theoretically the opposite should be true, at least for small surface charge densities ($\beta \sim 1\%$). Let us note that the method for determination of BLM surface charge used by us actually measures the surface potential difference and the calculation of σ_s from it presumes the validity of Gouy-Chapman theory, whose applicability to biological membranes with complicated dielectric profile has been questioned several times (Vaidhyanathan 1982, 1983).

The comparison between the theory and the experiment reveals the decisive role of the contribution from the surface charge equilibrium shift compared to all other contributions. The values of $\mathrm{d}\beta/\mathrm{d}A$ and β are not directly connected, but membranes with very low surface charge at isoelectric conditions should display one to two orders of magnitude smaller flexoelectric signals, of dipolar origin. This was probably the case with the weak, poorly reproducible signals from some very fresh PE/n-decane preparations.

The linear relationship between the mechano-electric signals and the membrane curvature down to very low curvatures confirms the notion about its flexoelectric origin.

The negative signs of the flexo-coefficients f^F and f^B are in agreement with the theoretical expectations for negatively charged lipid heads becoming increasingly negative on raising the area per lipid head.

The frequency dependence of the amplitude of the signal is in agreement with the flexoelectric theory. The limiting frequency, $\nu_{\mathrm{lim}} \sim 150$ Hz, gives for the first time information about the rate of the lateral lipid exchange in a BLM-torus system. The partial or complete disappearance of the first harmonic at ν_{lim}, especially at low ionic strength probably has something to do with the interference of both regimes of membrane polarization.

The high frequency limit of the relative phase of 270° is in agreement with the theoretical value of $3\,\pi/2$ (3.16). The low frequency limit of 140° is a little lower than the theoretical $-\pi/2$ (3.15). The gradual transition of the phase between these two limiting values is an indication about the gradual switching between the two mechanisms of membrane polarization when increasing the frequency.

The negative sign of the flexo-coefficients is in agreement with the negative surface charge and with the monolayer data showing that by increasing the area per head it becomes more negative.

Considering the characteristic thickness dependence of various multipole contributions (3.9) one can conclude that the charge contribution to the measured current is proportional to the thickness, while the dipolar one is thickness-independent. Control measurements on a thinner, solvent-free BLM (PE/squalene, $d = 2.7$ nm) showed a drastic decrease of the signal in both regions. This again indicates the role of charges. On the other hand, flexoelectric signals were also registered from coloured decane BLM's in the course of their thinning, but their amplitude was not very much higher than in the black state. This could be an indication of a dipole contribution. However, this apparent controversy can be easily resolved by realizing that the central region of a thick, coloured membrane is filled by isotropic solvent. Such a structure does not bend as a solid (or liquid crystal) shell but both monolayers

behave as though uncoupled and the overall thickness is unimportant.

The bending-induced surface charge equilibrium shift, $d\beta/dA$, does not directly depend on the surface charge value β, and β itself has only a small effect upon f^C, thus explaning the lack of a marked influence of the surface charge variation. The ionic strength influence can be understood in terms of the increase of the slope and the non-linearity of $\beta(A)$ dependence in monolayers with decreasing ionic strength (a clue to this is given by Fig. 6 of Standish and Pethica (1968)) revealing again the contribution of surface charge variations. Surface dipole variations should be less sensitive to the ionic strength influence.

The influence of phloretin adsorption should be interpreted in terms of separation of ionisable PE molecules by non-ionisable phloretin molecules, thus decreasing the mutual influence of PE molecules and making their partial charge largely independent of the area per head group.

The lack of an effect of the membrane conductivity upon the current is indicative of its displacement character. On the other hand, the correlation between the background conductivity of a BLM and its flexoelectric signal (Passechnik and Bichkova 1978), together with our finding of signal enhancement in the stress state of the BLM before rupture is due, according to us, to a switch of the membrane polarization regime from blocked to free flip-flop because of the presence of hydrophilic pores (Derzhanski et al. 1981). The selective pushing of ions due to the hydrostatic pressure difference (Passechnik and Bichkova 1978) could not explain either the current amplitude or the phase shift between the curvature and the current oscillations and their frequency dependence.

6. Conclusion

The first detailed study of the dynamics of the curvature-electric effect in BLM is reported. Two regimes of this effect (a low frequency one and a high frequency one) are revealed. The relation of the effect to the membrane flexoelectricity phenomenon is discussed in detail. A new flexoelectric mechanism (i.e. curvature-induced shift of the surface charge equilibrium) is proposed, its contribution is estimated and its decisive role is demonstrated. The flexoelectric coefficients of a phosphatidylethanolamine/n-decane membrane in KCl electrolyte are evaluated both in the low and in the high frequency regime.

Important biological implications of the flexoelectric effect in curved biomembrane structures (active and passive ion transport, lateral distribution of membrane proteins, membrane contact, shape of erythrocytes etc.) have been discussed elsewhere (Petrov 1975, 1977; Petrov et al. 1978; Petrov 1978; Petrov et al. 1979; Bivas and Petrov 1981; Petrov 1984; Seleznev and Petrov 1983; Petrov and Bivas 1984).

Further development of these ideas would essentially rely upon the new information about model systems gained in the present study. But an actual task would also be to study the flexoelectric effect in a real biomembrane by using the concepts advanced in this work.

Acknowledgements. We would like to acknowledge very stimulating discussions with Prof. Yu. A. Chizmadzhev, Prof. V. S. Markin, Dr. I. G. Abidor and Dr. V. F. Pastushenko. A. G. Petrov is thankful to Prof. Yu. A. Chizmadzhev and his coworkers for the generous hospitality during the stay in the Institute of Electrochemistry.

References

Andersen OS, Finkelstain A, Katz I, Cass A (1976) Effect of phloretin on the permeability of thin lipid membranes. J Gen Physiol 67: 749–771

Bivas I, Petrov AG (1981) Flexoelectric and steric interactions between two lipid bilayer membranes resulting from their curvature fluctuations. J Theor Biol 88: 459–483

Cherni VV, Sokolov VS, Abidor IG (1980) Determination of surface charge of bilayer lipid membranes. Bioelectrochem Bioenerg 7: 413–420

Chizmadzhev YuA, Chernomordik LV, Pastushenko VF, Abidor IG (1982) Electrical breakdown of BLM. In: Kostyuk PG (ed) Biofizika membran, vol 2, VINITI, Moscow, pp 161–266

DeGennes PG (1974) The physics of liquid crystals. Claredon Press, Oxford

Derzhanski A, Petrov AG, Pavloff YV (1981) Curvature-induced conductive and displacement currents through lipid bilayers. J Phys Lett (Paris) 42: L-119–L-122

Lis LJ, McAlister M, Fuller N, Rand RP, Parsegian VA (1982) Measurement of the lateral compressibility of several phospholipid bilayers. Biophys J 37: 667–672

Meyer RB (1969) Piezoelectric effects in liquid crystals. Phys Rev Lett 22: 918–922

Ochs AL, Burton RM (1974) Electrical response to vibration of a lipid bilayer membrane. Biophys J 14: 473–489

Passechnik VI, Bichkova EJ (1978) Piezoeffect, background conductivity and filtration coefficients of bilayer lipid membranes. Biofizika (Moscow) 23: 551–552

Passechnik VI, Sokolov VS (1973) Permeability change of modified bimolecular phospholipid membranes accompanying periodical expansion. Biofizika (Moscow) 18: 655–660

Passechnik VI, Sokolov VS (1975) Mechanical oscillations of bilayer membranes. Biofizika (Moscow) 20: 743–744

Petrov AG (1975) Flexoelectric model for active transport. In: Physical and chemical bases of biological information transfer. Plenum Press, New York London, pp 111–125

Petrov AG (1977) Flexoelectric effects and transport phenomena in biomembranes. Fourth Winter School Biophys Mem-

brane Transport, Poland, School Proceedings, Wroclaw, 3:168–176

Petrov AG (1978) Mechanisms of curvature-induced membrane polarization and their influence on some membrane properties. Studia biophys 74:51–52, Microfiche 4/pp 14–25

Petrov AG (1984) Flexoelectricity of lyotropics and biomembranes. Nuovo Cimento 3D:174–192

Petrov AG, Bivas I (1984) Elastic and flexolelectric aspects of out-of-plane fluctuations in biological and model membranes. Prog Surf Sci 16:389–512

Petrov AG, Derzhanski A (1976) On some problems in the theory of elastic and flexoelectric effects in bilayer lipid membranes and biomembranes. J Phys (Paris) (Suppl) 37:C3-155–C3-160

Petrov AG, Pavloff YV (1979) A new model for flexoelectric polarization of bilayer lipid membranes at blocked "flip-flop". J Phys (Paris) (Suppl) 40:C3-455–C3-457

Petrov AG, Tverdislov VA, Derzhanski A (1978) Flexoelectric aspects of lipid-protein interaction in biomembranes. Ann Phys (Paris) 3:273–274

Petrov AG, Seleznev SA, Derzhanski A (1979) Principles and methods of liquid crystal physics applied to the structure and functions of biological membranes. Acta Phys Pol A55:385–405

Seleznev SA, Petrov AG (1983) Short and long-range interactions between proteins and mesomorphic lipids within biological membranes. CR Acad Bulg Sci 36:615–618

Shipley GG (1973) Recent X-ray diffraction studies of biological membranes and membrane components. In: Chapman D, Wallach DFH (eds) Biological membranes, vol 2. Academic Press, London, pp 1–89

Sokolov VS (1982) Investigation of charge transfer mechanism through a membrane, induced by nigericin and grisorixin antibiotics. PhD Thesis, Moscow State University

Sokolov VS, Cherni VV, Markin VS (1984) Measurement of the dipolar potential jumps at the adsorption of phloretin on the BLM surface by the inner field compensation method. Biofizika (Moscow) 24:424–429

Standish MM, Pethica BA (1968) Surface pressure and surface potential study of a synthetic phospholipid at the air/water interface. Trans Faraday Soc 64:1113–1122

Szekely JG, Morash BD (1980) The effect of temperature on capacitance changes in an oscillating model membrane. Biochim Biophys Acta 599:73–80

Taupin C, Dvolaitzky M, Sauterey C (1975) Osmotic pressure induced pores in phospholipid vesicles. Biochemistry 14:4771–4775

Vaidhyanathan VS (1982) Inhomogeneous interfacial regions near a cell surface. Studia biophys 90:37–46

Vaidhyanathan VS (1983) ADO and additional comments on the inhomogeneous regions, near a biological membrane. 7th Int Symp Bioelectrochemistry, Stuttgart, FRG

Wobschall D (1971) Bilayer membrane elasticity and dynamic response. J Colloid Interface Sci 36:385–396